


CASE REPORT

Phenotypic spectrum in a family with a novel *RAC2* p.I21S dominant-activating mutation

Louisa Ashby¹, Lydia Chan², Christine Winterbourn¹, See-Tarn Woon³, Paula Keating⁴, Raoul Heller⁵, Rohan Ameratunga^{2,3}, Ignatius Chua^{4,6} & Kuang-Chih Hsiao^{7,8} 

¹Mātai Hāora – Centre for Redox Biology and Medicine, Department of Pathology and Biomedical Science, University of Otago Christchurch, Christchurch, New Zealand

²Department of Clinical Immunology, Auckland City Hospital, Auckland, New Zealand

³LabPLUS, Te Toka Tumai, Te Whatu Ora, Auckland, New Zealand

⁴Canterbury Health Laboratories, Te Whatu Ora, Christchurch, New Zealand

⁵Genetic Health Service NZ – Northern Hub, Te Toka Tumai, Auckland, New Zealand

⁶Christchurch Hospital, Te Whatu Ora, Christchurch, New Zealand

⁷Starship Child Health, Te Whatu Ora, Auckland, New Zealand

⁸Department of Paediatrics: Child and Youth Health, Faculty of Medical and Health Sciences, University of Auckland, Auckland, New Zealand

Correspondence

K-C Hsiao, Department of Paediatrics: Child and Youth Health, Faculty of Medical and Health Sciences, University of Auckland, Auckland, New Zealand.

E-mail: kc.hsiao@auckland.ac.nz

Received 5 January 2024;

Revised 11 February 2024;

Accepted 12 February 2024

doi: 10.1002/cti2.1493

Clinical & Translational Immunology
2024; 13: e1493

Abstract

Objectives. Dominant-activating (DA) lesions in *RAC2* have been reported in 18 individuals to date. Some have required haematopoietic stem cell transplantation (HSCT) for their (severe) combined immunodeficiency syndrome phenotype. We aimed to investigate clinical and cellular features of a kindred harbouring a novel variant in *RAC2* p.Ile21Ser (I21S) to better understand DA lesions' phenotypic spectrum. **Methods.** Clinical and immunological information was collated for seven living individuals from the same kindred with *RAC2* p.I21S. We evaluated neutrophil morphology, *RAC2* protein expression and superoxide production using freshly isolated neutrophils stimulated with phorbol-12-myristate-13-acetate (PMA) and N-formyl-MetLeuPhe (fMLP). **Results.** Patient 1 (P1, aged 11, male) has a history of bacterial suppurative otitis media, viral and bacterial cutaneous infections. P1's siblings (P2, P3), mother (P4), maternal aunt (P5) and uncle (P6) have similar infection histories. P1's maternal cousin (P7) presented with Burkitt's lymphoma at age 9. All affected individuals are alive and none has required HSCT to date. They have chronic lymphopenia affecting the CD4⁺T and B-cell compartments. P1–3 have isolated reduction in IgM levels whereas the adults universally have normal immunoglobulins. Specific antibody responses are preserved. Affected individuals have neutrophil vacuolation, and their neutrophils have enhanced superoxide production compared to healthy controls. **Conclusion.** *RAC2* p.I21S is an activating variant causing notable morphological and functional abnormalities similar to other reported DA mutations. This novel variant expands the broad clinical phenotypic spectrum of *RAC2* DA lesions, emphasising the need

to tailor clinical management according to patients' disease phenotype and severity.

Keywords: combined immunodeficiency, dominant-activating mutation, phenotypic spectrum, RAC2

INTRODUCTION

Ras-related C3 botulinum toxin substrate 2 (RAC2) belongs to the Ras homology family of guanosine triphosphatases (GTPases) and is exclusively expressed in haematopoietic cells. RAC2 has vital physiological roles including NADPH oxidase activation, actin polymerisation, cytoskeleton reorganisation, gene transcription, cell survival and cell adhesion.¹ There are many identified mutations in small GTPase proteins across the broad superfamily of Ras homology (RHO) GTPases, often associated with complex immunological effects.²

Dominant-activating (DA) mutations in the RAC2 gene were first described in 2019 and to date, seven unique DA mutations have been identified.^{3–10} Affected individuals present with (severe) combined immunodeficiency (CID) syndrome with some requiring haematopoietic stem cell transplantation (HSCT). Herein, we present the features of seven individuals from the same kindred with a novel DA variant in RAC2 (c.62T > G, p.I215) (Figure 1a).

RESULTS

Case report

Clinical and immune features of affected individuals are summarised in Table 1. Patient 1 (P1, aged 11, male) presented in early childhood with recurrent or atypical infections including suppurative otitis media (*Streptococcus pyogenes*, *Haemophilus influenzae*, *Staphylococcus aureus*), bacterial conjunctivitis (*Staphylococcus aureus*), viral and bacterial cutaneous infections (*Herpes simplex virus 1*, *Molluscum contagiosum*, *Staphylococcus aureus*, *Streptococcus pyogenes*), and infectious gastroenteritis (*Salmonella*, *Giardia*, *Campylobacter*). He continues to respond well to empiric antimicrobials and has never required hospitalisation. P1's two siblings (P2, aged 13, male; P3, aged 10, female) have similar infection

histories but overall milder in severity. P1's mother (P4, aged 46) has recurrent sinopulmonary and bacterial and viral skin infections since childhood. She has two similarly affected siblings, one with a milder phenotype (P5, aged 42, female) and another with more severe disease complicated by bronchiectasis (P6, aged 51, male). P4 has two other siblings who are healthy. While sinopulmonary infections continued into adulthood for P4–6, each were briefly hospitalised for treatment of community-acquired pneumoniae on 1–2 occasions, the frequency of cutaneous infections has reduced over time. P1's maternal cousin (P7, aged 11, son of P5) has no significant infection history but presented with Burkitt's lymphoma at age 9. He went into remission following chemotherapy but requires immunoglobulin replacement because of severe hypogammaglobulinemia. P1's late maternal grandmother (P8) was reported to have a lifelong history of recurrent sinopulmonary and cutaneous infections and multifocal destructive osteomyelitis. She succumbed to metastatic squamous cell carcinoma of the scalp at age 69. No patient in this kindred had clinical features of autoimmunity or mucocutaneous candidiasis.

All affected individuals display chronic lymphopenia affecting the CD4⁺T and B-cell compartments, with an expanded proportion of gamma-delta double-negative T cells (Table 1). At birth, P1 and P2 had low T-cell receptor excision circles (TRECs) which remain low (P1 at birth, 6; at present, 17; P2 at birth, 9; at present, 4; laboratory's neonatal cut-off > 18). P3's TRECs are normal (at birth, 30; at present, 21). In all three, CD4⁺ naïve (CD45RA⁺/CD62L⁺) T cells are present (currently P1 34.9%, P2 37.1%, P3 55.1% as a % of CD4⁺ T cells) and lymphocyte proliferative response to mitogens is preserved. The children have isolated reduction in IgM levels whereas the adults universally show normal immunoglobulins. Specific antibody responses to protein and viral antigens, including to SARS-CoV-2 mRNA vaccine, are preserved. Taken together, the clinical and

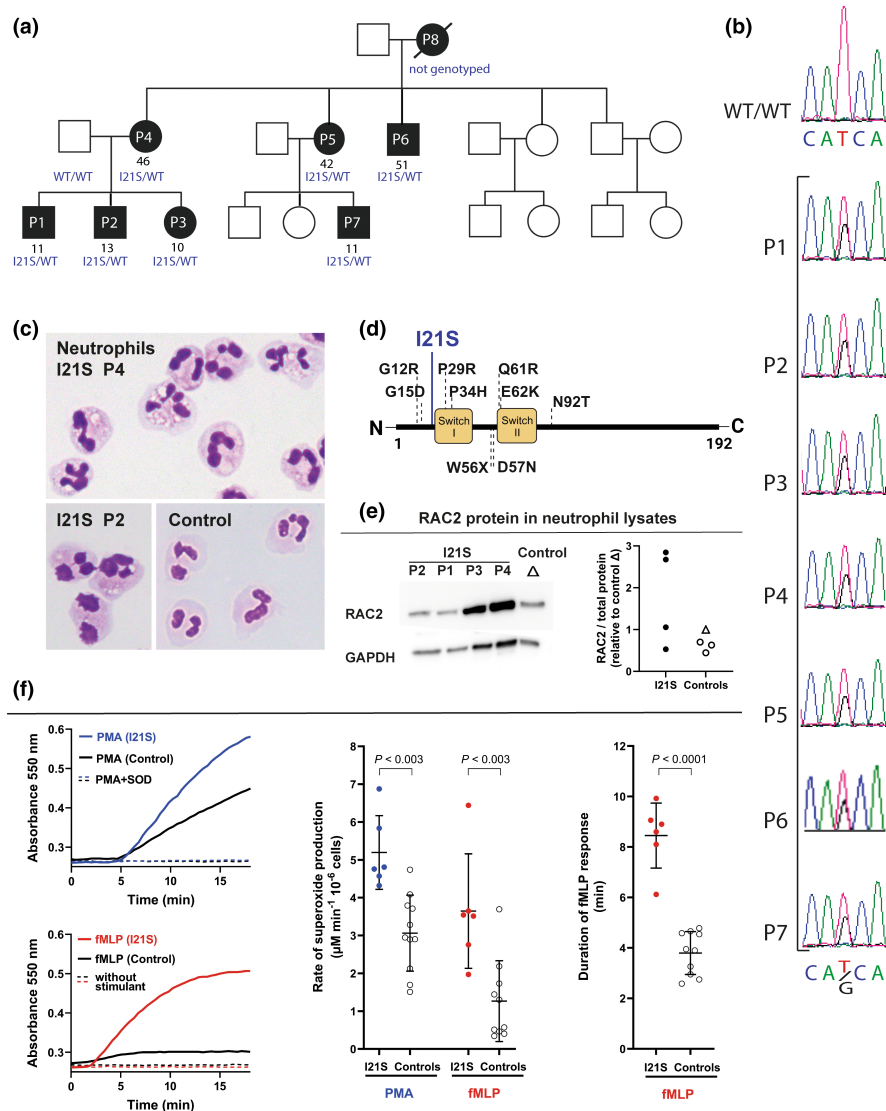


Figure 1. RAC2 p.I21S is a dominant-activating mutation. **(a)** Pedigree, **(b)** Sanger sequencing of variant compared to wild-type (WT) sequence of the father of P1-P3, **(c)** neutrophils from P2 and P4 showing vacuolation, **(d)** amino acid location of reported DA mutations (above line), and negative effect mutations (below line), and **(e)** Western blot signals for RAC2 protein (and loading control GAPDH) in neutrophil lysates of four family members and four unrelated healthy controls. Quantification was normalised for loading and is relative to the travel control (Δ). **(f)** Neutrophil superoxide production monitored by reduction of cytochrome c at 550 nm. Representative traces from one family member and the same-day control (black) stimulated with 100 ng mL⁻¹ PMA (blue) and 100 nM fMLP (red). Rates of production, and duration of the fMLP burst, are compared for all RAC2 p.I21S individuals and controls.

immunological phenotypes of affected individuals are consistent with a combined immunodeficiency syndrome.

Genotyping

Further evaluation using next-generation sequencing (clinical grade comprehensive primary immunodeficiency gene panel) identified a

heterozygous missense variant of RAC2 (c.62T > G, p.I21S) in P1 (Figure 1b). The variant has not been observed in a large reference population cohort (gnomAD). *In silico* tools predicted the variant to be disease causing (MutationTaster), not tolerated (SIFT) and probably damaging (PolyPhen2), with a CADD score of 29.6. Sanger sequencing confirmed presence of the variant in all affected individuals (P1 to P7), and absence in the unaffected father

Table 1. Clinical manifestations and immunologic evaluation of affected individuals

Current age	P1		P2		P3		P4		P5		P6		P7		P8	
	11 years	13 years	10 years	46 years	42 years	51 years	11 years	69 years								
RTI – V	+	+++	+++	+++	+++	+	+	+	+	+	+	+	+	+	+	+++
RTI – B	0	+	+	+, x	+, x	+	+	+	+	+	+	+	+	+	+	+++
MCI – V	+++	+++	+++	+	+	+	+	+	+	+	+	+	+	+	+	+++
MCI – B	+++	+++	+	0	0	0	0	0	0	0	0	0	0	0	0	+++
MCI – F	+	0	0	+	+++	0	+	+	+	+	+	+	+	+	+	0
GI	0	0	+	+	0	0	+	+	0	0	0	+	+	+	+	0
Malignancy	0	0	0	0	0	0	0	0	0	0	0	0	0	0	0	+
Age at evaluation	3 years	11 years	8 years	12 years	5 years	9 years	43 years	40 years	48 years	49 years	9 years	10 years	10 years	9 years	10 years	NA
IgG (g L ⁻¹)	6.6	9.2	9.2	9.2	7.3	9.2	9.5	10.1	7.4	7.4	9.3	9.8	4.0 ^c	4.0 ^c	7.0	-
IgA (g L ⁻¹)	1.1	0.5	0.5	0.5	0.4	1.1	1.7	1.8	1.4	1.4	1.4	1.4	0.7	0.7	0.4	-
IgM (g L ⁻¹)	0.28^a	0.07^b	0.12^c	0.07^b	0.5	0.1^c	0.6	0.7	1.2	1.2	1.0	1.0	0.4^c	0.4^c	0.1^b	-
CD4 ⁺ T cells (μL ⁻¹)	196 ^f	144 ^g	146 ^g	133 ^g	361 ^f	247 ^g	200 ^h	-	180 ^h	180 ^h	190 ^h	140 ^h	110 ⁱ	110 ⁱ	235 ⁱ	-
CD8 ⁺ T cells (μL ⁻¹)	482	337	354	354	398	284	300	-	710	710	460	210	100 ^j	100 ^j	347	-
B cells (μL ⁻¹)	171	91	73 ^g	73 ^g	142	106	20 ^h	-	30 ^h	30 ^h	160	9 ^h	-	-	175	-
Naïve CD4 ⁺ /CD45RA ⁺ /62L ⁺ (% of CD4 ⁺)	-	34.9	43.8	37.1	59.5	55.1	-	-	-	-	-	-	-	-	35.1	-
Naïve CD8 ⁺ /CD45RA ⁺ /62L ⁺ (% of CD8 ⁺)	-	28.8	30.8	20.4	58.9	50.5	-	-	-	-	-	-	-	-	31.2	-
γδ DNT (% of T cells)	-	20.5 ^j	11.2 ^j	14.3 ^j	17.3 ^j	17.3 ^j	-	-	-	-	-	-	-	-	-	-
αβ DNT (% of T cells)	-	1.5	2.1	2.1	↑	↑	-	-	-	-	-	-	-	-	-	-
Naïve B cells CD27 ⁻ /IgD ⁺ (% of B cells)	87.8 ^k	93.8 ^k	92.6 ^k	94.0 ^k	91.4 ^k	90.9 ^k	-	-	-	-	-	-	-	-	98.1 ^k	-
Switched memory B cells CD27 ⁻ /IgD ⁻ (% of B cells)	6.9	1.5 ^k	1.7 ^k	1.8 ^k	3.4 ^k	2.3 ^k	-	-	-	-	-	-	-	-	< 1.0 ^k	-
Median TREC at birth	-	6 ^l	9 ^l	9 ^l	-	30	-	-	-	-	-	-	-	-	-	-
TREC at present	-	17 ^l	4 ^l	4 ^l	-	21	-	-	-	-	-	-	-	-	-	-
Naïve CD4 ⁺ T cells (×10 ⁶ L ⁻¹)	-	50 256	49 343	136 097	-	-	-	-	-	-	-	-	-	-	-	-
T-cell profile (mitogens)	N	-	N	-	N	-	-	-	-	-	N	-	-	-	N	-

(Continued)

Table 1. Continued.

	P1	P2	P3	P4	P5	P6	P7	P8
Current age	11 years	13 years	10 years	46 years	42 years	51 years	11 years	69 years
T-cell profile (antigens)	↓	↓	↓	—	—	—	—	↓
Ab response (prt antigens)	—	N	N	—	—	—	—	—
Ab response (poly-sacch)	↓	↓	↓	—	—	↓	—	—
Ab response (HSV, VZV)	N	N	N	—	—	—	—	—
SARS-CoV-2	—	Weak	—	Weak	—	—	Strong	—
RBD-response	—	—	—	—	Strong	—	—	Absent*

*On immunoglobulin replacement therapy. Reference ranges: a [IgG 3.0–11.2, IgA 0.29–1.69, IgM 0.4–1.8]; b [IgG 6.0–15.0, IgA 0.3–2.4, IgM 0.4–1.8]; c [IgG 5.0–13.3, IgA 0.3–2.4, IgM 0.4–1.8]; d [IgG 5.0–13.3, IgA 0.29–1.69, IgM 0.4–1.8]; e [IgG 6.0–15.0, IgA 0.8–4.0, IgM 0.4–2.5]; f LabPLUS Auckland [CD4 500–2400, CD8 300–1600, CD19 200–2100]; g LabPLUS Auckland [CD4 500–1650, CD8 210–1200, CD19 80–600]; h Canterbury Health Laboratories [CD4 300–1400, CD8 200–900, CD19 100–500]; i Canterbury Health Laboratories [CD4 300–2000, CD8 300–1800, CD19 200–1600]; j > 2.5% abnormal; k Naïve B cells 57.7–79.7%, Switched memory B cells 5–21%, I TRECs neonatal cut-off > 18. 0, none; +, infrequent (< 2/year, without use of prophylactic antimicrobials); ++, infrequent (< 2/year, with use of prophylactic antimicrobials); +++, frequent (≥ 2/year); ↑, increased; ↓, reduced; →, not tested; Ab, antibody; B, bacterial; F, fungal; GI, gastrointestinal infection; HSV, herpes simplex virus; Ig, immunoglobulin; MCI, mucocutaneous infection; N, normal; NA, not applicable; poly-sacch, poly-saccharides; prolif, proliferation; prt, protein; RBD, receptor-binding domain; RTI, respiratory tract infection; TREC, T-cell receptor excision circles; V, viral; VZV, varicella zoster virus; x, hospitalised; γδ DNT, gamma-delta double-negative T cells. Bold arrows indicate results are outside of reference ranges.

(WT/WT of Figure 1a and b) of P1, P2 and P3. Genetic material for P8 was not available. The novel variant is in the N-terminal region of the protein and is proximate to other DA mutations near the so-called structure–function related Switch domains (Figure 1d).

The comprehensive primary immunodeficiency gene panel identified only two other novel genetic variants in the proband (one heterozygous *AIRE* c.560C > T, p.Ser187Leu missense variant with a CADD score of 24.9 and one heterozygous *ZNF341* c.121C > T, p.Pro41Ser missense variant with a CADD score of 5.7). No patient in this kindred had clinical features of disease classically associated with harbouring biallelic pathogenic mutations in either of these genes.

Neutrophil studies

RAC2 is essential for neutrophil NADPH oxidase activation and superoxide production therefore we evaluated the impact of RAC2 p.I21S variant on neutrophil morphology and RAC2 protein expression. As seen with other DA mutations, ^{3,5,9,10} light microscopy of patients’ neutrophils showed increased vacuolation (Figure 1c). Western blotting for RAC2 in neutrophil lysates from four of the family members plus controls (Figure 1e), showed a single band for RAC2 in all samples. Levels varied between RAC2 p.I21S individuals but were not less than normal.

Production of superoxide was measured using freshly isolated neutrophils stimulated with phorbol-12-myristate-13-acetate (PMA) and N-formyl-MetLeuPhe (fMLP) (Figure 1f). With PMA, neutrophils from healthy controls gave the expected extended burst of superoxide-dependent cytochrome c reduction while neutrophils from RAC2 p.I21S patients showed a significantly higher rate of superoxide generation. As shown, stimulation of normal neutrophils by fMLP typically gives a short burst of superoxide production at a lower rate than with PMA. In contrast to controls, superoxide production by the RAC2 p.I21S cells lasted significantly longer. Taken together, these findings showed that the RAC2 p.I21S mutation causes heightened NADPH oxidase activation in neutrophils. The mutation does not cause constitutive activation of NADPH oxidase, rather it appears that RAC2 p.I21S supports extended ‘switched on’ mode for both stimulants tested.

This is consistent with increased activation observed in neutrophils with other RAC2 DA mutations,^{3,4,9,10} and confirms that RAC2 p.I21S is a DA lesion. These results from patients' neutrophils suggest it is unlikely that defective NADPH oxidase activity is responsible for the prevalent infections in these patients.

DISCUSSION

With the inclusion of our cohort, there are now a total of 25 individuals (8 adults and 17 children) reported globally to have pathogenic RAC2 DA variants, exhibiting significant phenotypic heterogeneity (Figure 2). Two RAC2 variants (p.G12R,⁸ p.Q61R⁷) affecting four individuals have been associated with SCID with patients presenting with sepsis around birth and needing HSCT in the first 3 months of life.

Our novel RAC2 variant (p.I21S) joins other variants (p.G15D,¹⁰ p.P29R,⁹ p.P34H,⁴ p.E62K,^{3,6} p.N92T⁵) that are associated with early-life-onset CID of variable expressivity (now *n* = 21). Of the 6 cases with p.E62K variant, three successfully received HSCT and two received lung transplantation. One case with p.N92T variant received two HSCT aged 9 but ultimately succumbed to disseminated adenovirus infection.

The mechanisms underlying the adaptive immunity defects, including our patients' combined immunodeficiency syndrome, in RAC2 DA mutations remain elusive although actinopathy and pro-apoptosis have been postulated. Reported effects of the mutated RAC2 protein in lymphoid cells include F-actin accumulation, impaired actin polymerisation, dysregulated cytokine production, accumulation of senescent CD8⁺CD57⁺ T cells, accelerated T- and

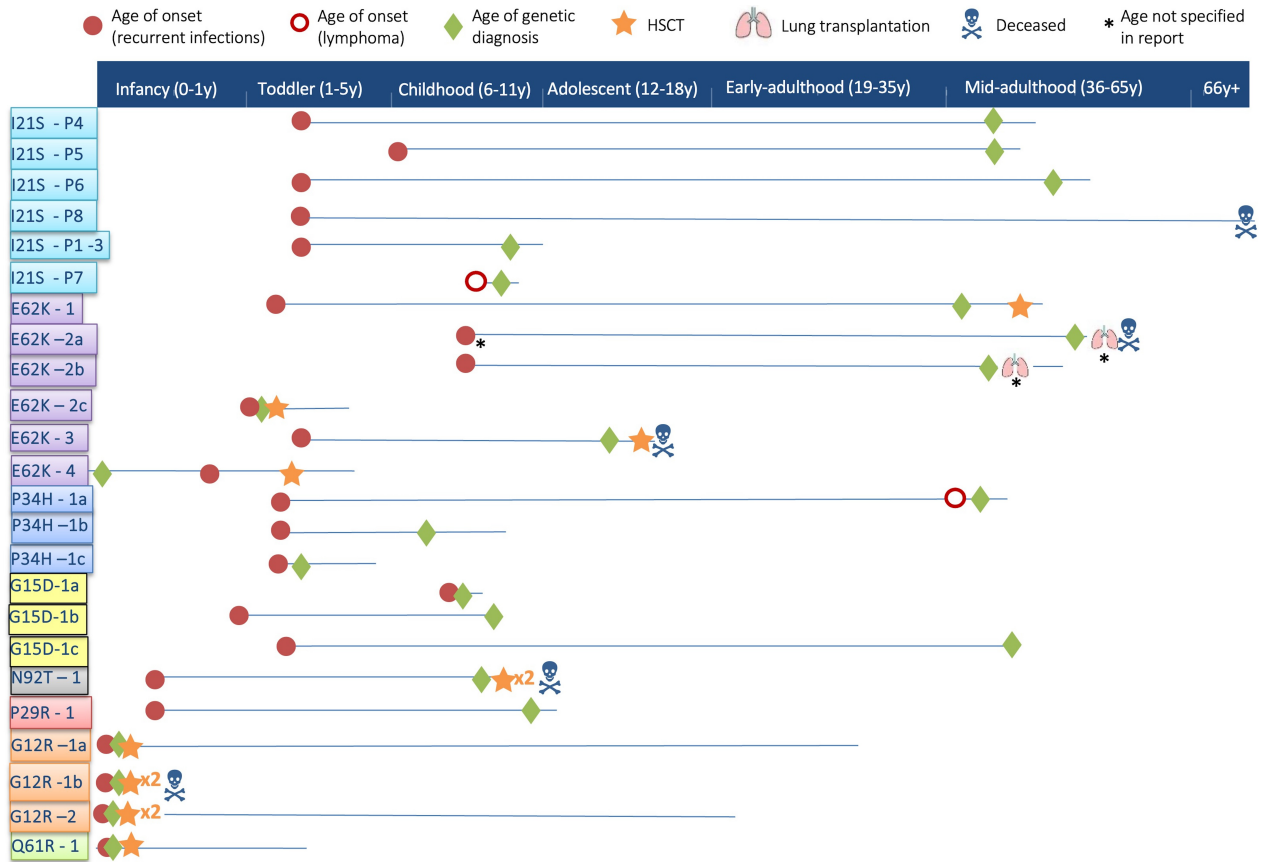


Figure 2. Phenotypic spectrum of reported RAC2 dominant activating mutations. A schematic timeline of natural history and disease evolution demonstrating the phenotypic spectrum of RAC2 dominant activating mutations. Each line represents a patient or a cluster of patients identified by their RAC2 mutation. Patients are clustered if they have similar clinical histories. The different symbols (see key at top) represent the age of onset of recurrent infections, lymphoma, genetic diagnosis, haematopoietic stem cell transplant (HSCT), lung transplantation, and age of death. The asterisk indicates instances where the age of the specific event was not specified in the original report (references given in text). Some individuals received more than one HSCT as indicated by the number adjacent to the orange star.

B-lymphocyte apoptosis, and functional and developmental alteration in NK cells.^{4,9,10}

Additionally, we observed in our patients an expanded gamma-delta double-negative T-cell population. Gamma-delta T cells are generally thought to serve as the first line of defence in epithelial and mucosal tissues owing to their ability to rapidly respond to pathogens in a major histocompatibility complex independent manner.¹¹ Increased numbers of gamma-delta T cells in the context of a CID may be advantageous in partially rescuing the immune phenotype associated with carrying *RAC2* DA mutations and warrant further investigation.

Overall, our cohort presented with a phenotype that was milder than other reported variants, with no individual requiring HSCT to date. In this kindred, infection frequency associated with the CID seems to reduce over time suggesting development of compensatory mechanisms. This p.I21S variant expands the phenotypic spectrum of *RAC2* DA lesions, emphasising the need to tailor clinical management according to patients' disease phenotype and severity.

METHODS

Blood collection and analyses

During this study, patients received medical care in Auckland, or Christchurch, New Zealand. Standard procedures were followed for all NATA-accredited clinical laboratory tests including genotyping services. For all immune biomarkers, results were interpreted against validated reference ranges where available, see Table 1 footnotes.

In Christchurch's clinical laboratory (Canterbury Health Laboratories), lymphocyte proliferation to stimulus was quantified by measuring the dilution of an intracellular dye label (CFSE) in the stimulated cells by flow cytometry. Cells were separated from blood using Lymphoprep (STEMCELL Technologies, Vancouver, Canada). PBMC were labelled with CFSE and cultured with the mitogens phytohaemagglutinin (PHA), Concanavalin A (ConA), poke weed mitogen Soluble OKT3 (PWM) and Tetanus toxoid (TT). After culturing for 3 days with mitogens and 7 days with TT, cells were labelled with CD3-APC and 7AAD. The proportion of live T cells, CD3-positive 7AAD-negative cells, with a diluted CFSE signal (indicative of proliferation) was determined by flow cytometry. Percentage of live CD3 cells that underwent more than one cell division following stimulation with various agonists was considered abnormal if less than three times normal for two or more mitogens.

In Auckland's clinical immunology laboratory (LabPLUS), lymphocyte proliferation studies were undertaken by ³H-thymidine (tritiated thymidine) uptake by proliferating lymphocytes stimulated with lectins (PHA, PWM, ConA) and antigens (tetanus and diphtheria toxoids and candida).

Responses to PHA and ConA were assessed at day 3 and the responses to PWM and antigens were assessed at day 7. Proliferation indices were derived from unstimulated background counts for each test.¹² Lymphocyte subsets were enumerated by flow cytometry to T (CD2, CD3) and B-cell antigens (CD19, CD20) and Natural Killer cells (CD16, CD56). Increased proportions of double-negative T (DNT) cells found during standard lymphocyte subset enumeration were further investigated by TCR- $\alpha\beta$ and TCR- $\gamma\delta$ staining.

T-cell receptor excision circles (TREC) were measured in New Zealand's national newborn screening laboratory using Enlite Neonatal TREC kit (PerkinElmer, Turku, Finland), with a neonatal cut-off of > 18.

Genotyping details are provided in the Results section. Variant positions based on GRCh37/hg19 were used for CADD (combined annotation-dependent depletion) calculations.

For neutrophil function testing (superoxide production), patients travelled to Christchurch to provide samples for same day analysis. Cytospin slides were also prepared on freshly isolated neutrophils for Romanowsky-type staining (Diff-Quik from RAL Diagnostics, Martillac, France). In the case of *RAC2* protein measurement, it was necessary to transport the blood for analysis the next day. For all neutrophil studies, peripheral blood from consenting healthy adult donors was processed in parallel as same-day control samples, under ethical approval from the Southern Health & Disability Ethics Committee, New Zealand. Age-sex matching of controls was not possible for paediatric samples.

Receptor binding domain (RBD) assay for SARS-CoV-2 antibody response

Patient samples taken pre- and post-SARS-CoV-2 mRNA vaccination were compared in a homogenous mobility shift assay, the method is based on that previously described.¹³ In brief, fluorochrome-labelled RBD protein is used to bind antibody complexes in samples which are resolved by size exclusion high pressure liquid chromatography. The assay detects RBD-specific antibodies and the complexity of the chromatogram qualitatively reports on the degree of vaccination response in an individual.

RAC2 protein expression in neutrophils

Blood samples for this analysis (8 mL in EDTA vacutainer tubes, kept at room temperature) were drawn in Auckland and delivered to the Christchurch laboratory by overnight courier. Blood from a healthy donor in Auckland served as a travel control. Three additional day-old blood samples from other healthy donors were processed and analysed in the same way to address the normal biological variation between samples. A modified purification protocol was used for day-old blood; Ficoll centrifugation of the whole blood sample omitting the initial dextran step, followed by erythrocyte depletion using an ammonium chloride lysis buffer (144 mM NH₄Cl, 10 mM NH₄HCO₃, 10 mM KCl, 0.1 mM EDTA). This optimised the yield of day-old neutrophils and kept the contamination by other leukocytes to < 30%.

Lysates (4×10^7 cells/mL) were made by vortexing in solubilisation buffer (150 mM NaCl, 50 mM Tris HCl pH 8, 1% Nonidet P40, 0.5% sodium deoxycholate, 0.1% sodium dodecyl sulphate, SDS) containing protease inhibitors (Pierce tablet formulation, plus 50 mM EDTA, 1 mM phenylmethylsulfonyl fluoride), and stored at -80°C . The protein concentration of lysates was determined by Lowry assay (DC kit by Biorad, Hercules, USA) and samples were boiled 95°C for 5 min in reducing sample buffer prior to running on 12% SDS-PAGE gels. Standard techniques were applied for transfer to PVDF membrane, before blocking with 3% milk in Tris-buffered saline with 0.1% Tween20 and incubating with anti-RAC2 antibody (1 h with 1:500 PA5-88121 rabbit polyclonal, raised against RAC2 amino acids 100–192 by Invitrogen) or anti-GAPDH (1 h with 1:10 000 LF-PA10018 rabbit polyclonal by Ab Frontier) as loading control. Standard protocols were used for signal development (1 h with 1:10 000 goat anti-rabbit peroxidase by DAKO) followed by chemiluminescence (ECL Amersham kit from Cytiva, Little Chalfont, UK), and image capture (Uvitec Cambridge system). Image J software was used for densitometry analyses. Signal intensity was related both to total protein loading or to GAPDH (which gave similar results) and values are expressed relative to the travel control. Day-old blood samples from three additional unrelated controls were processed and analysed in the same way.

Superoxide production by neutrophils

Neutrophils were isolated from freshly drawn heparinised venous blood by the standard procedure of dextran sedimentation followed by Ficoll centrifugation and hypotonic lysis of contaminating erythrocytes.¹⁴ The purity of neutrophil isolation was typically $> 96\%$ as measured by flow cytometry using their characteristic forward/side scatter known to accurately report the neutrophil population.¹⁵ Because of the small volumes of paediatric blood available, the cytochrome c reduction assay was performed in flat-bottomed 96-well plates. Where larger blood volumes from adult patients and healthy controls were available, a cuvette assay was also performed in a spectrophotometer (Hitachi U-3900). Both methods measured ΔA_{550} and were proportional in amplitude, but as the rate of superoxide production was consistently slower for neutrophils in the plate than the 1-mL cuvette, only plate-reader results are reported for all.

Immediately prior to use, 96-well plates were incubated with heat-inactivated foetal calf serum (50% in phosphate buffered saline, PBS) for 1 h at 37°C followed by several washes with PBS, to eliminate surface stimulation of neutrophils during the assay. Neutrophils ($5 \times 10^5 \text{ mL}^{-1}$) in prewarmed Hanks' balanced salt solution containing $40 \mu\text{M}$ cytochrome c and $40 \mu\text{g mL}^{-1}$ catalase were dispensed for a final volume of $200 \mu\text{L}$ per well and A_{550} was monitored in a plate-reader (BioTek Synergy Neo2) at 37°C in the presence or absence of stimulant. Samples were assayed in triplicate wells, and the stimulants 100 ng mL^{-1} (162 nM) PMA or 100 nM fMLP were added by multichannel pipette and mixed at time 0. The control with $20 \mu\text{g mL}^{-1}$ superoxide dismutase confirmed that the observed absorbance change was specific to superoxide reduction of cytochrome c.

For stimulation by PMA and fMLP, the absorbance traces were analysed for maximum rate (slope). For fMLP, the duration of response refers to the time between the start of the response to the intercept point for tangents drawn from the initial maximal rate and steady state rate. The absorbance change recorded by the plate-reader was calibrated against the 1 mL cuvette assay using $\epsilon_{550} 41 100 \text{ M}^{-1} \text{ cm}^{-1}$ for cytochrome c reduction. Data points shown in Figure 1 are from all tested family members (P1–P6), and healthy adult donor controls ($n = 10–11$), and bars show mean \pm S.D. Significant differences between groups were determined by the unpaired *t*-test, two-tailed (GraphPad Prism software).

ACKNOWLEDGMENTS

We thank the patients, their families and their health care professionals for their participation in this study. We thank Detlef Knoll for performing TREC measurements and Amy Hsu and her colleagues at National Institutes of Health (NIH) for helpful discussions. We thank Starship Foundation (consumables) and Marsden Fund of the Royal Society of New Zealand (salary support for LA) for funding this study. Open access publishing was facilitated by The University of Auckland, as part of the Wiley - The University of Auckland agreement via the Council of Australian University Librarians.

AUTHOR CONTRIBUTIONS

Louisa Ashby: Conceptualization; data curation; formal analysis; investigation; methodology; visualization; writing – original draft; writing – review and editing. **Lydia Chan:** Data curation; formal analysis; investigation; visualization; writing – original draft; writing – review and editing. **Christine Winterbourn:** Investigation; methodology; resources; supervision; writing – review and editing. **See-Tarn Woon:** Formal analysis; visualization; writing – review and editing. **Paula Keating:** Formal analysis; investigation; writing – review and editing. **Raoul Heller:** Investigation; writing – review and editing. **Rohan Ameratunga:** Investigation; writing – review and editing. **Ignatius Chua:** Investigation; writing – review and editing. **Kuang-Chih Hsiao:** Conceptualization; data curation; formal analysis; funding acquisition; investigation; methodology; resources; supervision; writing – review and editing.

CONFLICT OF INTEREST

The authors declare no conflict of interest.

DATA AVAILABILITY STATEMENT

The data that support the findings of this study are available from the corresponding author upon reasonable request.

REFERENCES

- Lougaris V, Baronio M, Gazzurelli L, Benvenuto A, Plebani A. RAC2 and primary human immune deficiencies. *J Leukoc Biol* 2020; **108**: 687–696.
- Masri RE, Delon J. RHO GTPases: From new partners to complex immune syndromes. *Nat Rev Immunol* 2021; **21**: 499–513.
- Hsu AP, Donkó A, Arrington ME *et al.* Dominant activating RAC2 mutation with lymphopenia, immunodeficiency, and cytoskeletal defects. *Blood* 2019; **133**: 1977–1988.
- Lougaris V, Chou J, Beano A *et al.* A monoallelic activating mutation in RAC2 resulting in a combined immunodeficiency. *J Allergy Clin Immunol* 2019; **143**: 1649–1653.
- Sharapova S, Haapaniemi E, Sakovich I *et al.* Heterozygous activating mutation in RAC2 causes infantile-onset combined immunodeficiency with susceptibility to viral infections. *Clin Immunol* 2019; **205**: 1–5.
- Smits BM, Lelieveld PHC, Ververs FA *et al.* A dominant activating RAC2 variant associated with immunodeficiency and pulmonary disease. *Clin Immunol* 2020; **212**: 108248.
- Stern H, Donkó A, Shapiro T *et al.* A novel RAC2 variant presenting as severe combined immunodeficiency. *J Clin Immunol* 2021; **41**: 473–476.
- Lagresle-Peyrou C, Alichon A, Sadek H *et al.* A gain-of-function RAC2 mutation is associated with bone marrow hypoplasia and an autosomal dominant form of severe combined immunodeficiency. *Haematologica* 2021; **106**: 404–411.
- Zhang L, Chen Z, Li W *et al.* Combined immunodeficiency caused by a novel de novo gain-of-function RAC2 mutation. *J Clin Immunol* 2022; **42**: 1280–1292.
- Zhang L, Lv G, Peng Y *et al.* A novel RAC2 mutation causing combined immunodeficiency. *J Clin Immunol* 2023; **43**: 229–240.
- Lawand M, Dechanet-Merville J, Dieu-Nosjean M. Key features of gamma-delta T-cell subsets in human diseases and their immunotherapeutic implications. *Front Immunol* 2017; **8**: 761.
- Ameratunga R, McKee J, French J, Prestidge R, Fanslow W, Marbrook J. Molecular pathology of the X-linked hyper-immunoglobulin M syndrome: Detection of wild-type transcripts in a patient with a complex splicing defect of the CD40 ligand. *Clin Diag Lab Immunol* 1996; **3**: 722–726.
- Hock BD, McKenzie JL, Goddard L *et al.* Discrimination of anti-drug antibodies with neutralizing capacity in infliximab- and adalimumab-treated patients: Comparison of the homogeneous mobility shift assay and the affinity capture and elution assay. *Ther Drug Monit* 2018; **40**: 705–715.
- Magon NJ, Parker HA, Ashby LV *et al.* Analysis of neutrophil bactericidal activity. *Methods Mol Biol* 2020; **2087**: 149–164.
- Kremserova S, Nauseef WM. Isolation of human neutrophils from venous blood. *Methods Mol Biol* 2020; **2087**: 33–42.



This is an open access article under the terms of the [Creative Commons Attribution-NonCommercial-NoDerivs](https://creativecommons.org/licenses/by-nc-nd/4.0/) License, which permits use and distribution in any medium, provided the original work is properly cited, the use is non-commercial and no modifications or adaptations are made.